Acta of Bioengineering and Biomechanics
Vol. 18, No. 4, 2016

Original paper
DOI: 10.5277/ABB-00469-2015-03

Biomechanical analysis of asymmetric mesio-distal molar positions loaded by a symmetric cervical headgear

NATALYA KIZILOVA[1]*, ALLAHYAR GERAMY[2], YURIJ ROMASHOV[3]

[1] Warsaw University of Technology, Faculty of Power and Aeronautical Engineering, Warsaw, Poland.
[2] Tehran University of Medical Sciences, Dentistry Research Institute, Department of Orthodontics, Tehran, Iran.
[3] Kharkov National Polytechnical University, Faculty of Mechanical Engineering, Ukraine.

Purpose: The plane 2D model and 3d finite element model of the headgear attached to two molars with different mesio-distal location are studied to show the asymmetric mechanical effects produced by symmetrically loaded headgear. In daily dental practice the asymmetrical location of molars is usually ignored. *Methods:* Six 3D finite element models of a symmetric cervical headgear were designed in SolidWorks 2011. The models showed symmetric molar position (model 1), 0.5 to 2 mm of anterior-posterior molar difference (models 2–5) and a significant asymmetry with 10 mm of difference in the locations (model 6). The head gear was loaded with 3N of force applied at the cervical headgear. The forces and moments produced on terminal molars are assessed. *Results:* It is shown the difference between the forces acting at the longer and shorter outer arms of the headgear increases with increase in the distance. The significant numeric difference in the forces has been found: from 0.0082 N (model 1) to 0.0324 N (model 5) and 0.146 N (model 6). These small forces may produce unplanned distal tipping and rotation of the molars around their vertical axes. The most important funding was found as a clockwise yaw moment in the system when is viewed superio-inferiorly. The yaw moment has been computed between –0.646 N·mm (model 1) and –1.945 N mm (model 5). *Conclusions:* Therefore even small asymmetry in location of molars loaded by a symmetric cervical headgear will produce undesirable movement and rotation of the teeth that must be taken into account before applying the treatment.

Key words: *finite element method, force system, asymmetry, yaw moment, orthodontic tooth movement, headgear*

1. Introduction

Orthodontic headgear (HG) is an appliance attached to dental braces or a palatal expander that serves for correcting severe bite problems, to retracting maxillary teeth or reinforcing tooth anchorage during retraction. It consists of the inner bow fastened to the molars and the outer bow to which the force is applied (Fig. 1). Headgears are prescribed in daily practice and the outer bows are routinely adjusted according to the needs of the practitioner. The missing link in this problem is to ascertain the length of the inner bow ends at the end of the adjustment of the HG adjustment visit. HG has had many ups and downs since its introduction in orthodontics. The appliance was first introduced by Norman William Kingsley but virtually ignored by H. Angle, though it has been shown to be very effective in treating orthodontic patients. In 1944, Oppenheim described its mechanical principles and revived its use in dental practice. From Oppenheim to 1970 various approaches to the use of HG have been described [10]–[13], [21]. In a comprehensive paper [1], the importance of precise control of magnitude, direction, and duration of extraoral force for increased HG efficiency and effectiveness in treating malocclusions in the late mixed dentition period was demonstrated. Biomechanics of the HGs as force systems have been studied in a series of papers [2]–[5], [9], [14]–[17], [20], [22], [23], [25] by

* Corresponding author: Natalya Kizilova, Warsaw University of Technology, ul. Nowowiejska 24, 00-001 Warsaw, Poland. Tel: +48 796 454 217, e-mail: kizilova@icm.edu.pl
Received: September 18th, 2015
Accepted for publication: January 5th, 2016

applying classical mechanics balance equations of force and moment of force.

Production of extra oral forces [16], [17], [20], [23] by application of unilateral [15] bows has been studied and classification of rotation and extra oral force systems has been done [25]. Biomechanical guidelines for the HG application have been formulated [4] and the importance of individual biomechanics of growth has been shown [9]. A comparative analysis of the extraoral and intraoral appliances has been done [2], [14] and finite element method (FEM) was shown a useful tool for practicing dentists [3], [5]–[8], [22]. In spite of the classical mechanics approach, the FEM allows determination of the tooth displacement and rotation accounting for its geometrical shape and location of the rigid (bone) and soft (gum) tissues around the tooth, as well as structure of periodontal ligaments (PDL) connecting the root of the tooth and its bony socket.

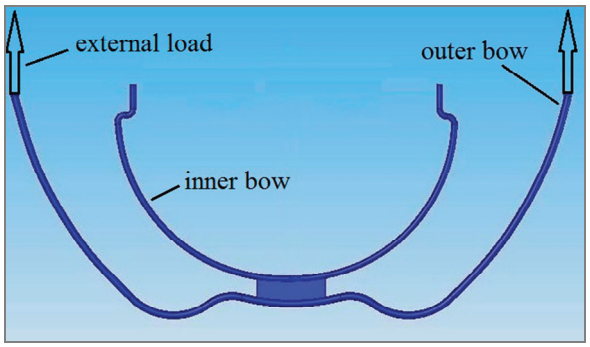

Fig. 1. Mechanical construction of the HG

A wealth of research has been done on the analysis of different lengths and positions of the outer bow. Analyses of the symmetrically and asymmetrically loaded outer bows revealed that with increasing asymmetry of the external loading the distal load to the power-arm side is accompanied by a shift of the lateral force and couple to the opposite side [6]–[8], [22]. In the cases when different molar distalization forces are needed on the right and left sides of the jaw, the unequal outer and inner bow configurations may be useful [3], [7], [22]. When the difference between the long and short outer bows is 40 mm, the forces produced at the long-side and short-side molars are in ratio 7:3 [3].

In some cases, the molars are not in the same mesio-distal position, regardless of how the symmetric cervical HG is adjusted. When the individual medio-lateral location of the molars is asymmetrical, significant difference in the forces produced could produce undesirable asymmetric displacement and rotation of the molars [7]. Clinically, it is often difficult to ascertain the mesio-distal and medio-lateral asymmetry of the molars on the left and right sides.

The effects of shortening of one outer bow was examined and evaluated by 3D FEM analysis [6]. It was shown that different forces resulted on the left and right molars, and a yaw moment in the system was produced resulting in a rotation about vertical axis. The FEM modeling of effects of unilateral expansion of the outer bow also revealed a yaw moment rotating the system [8]. It means that there are some structural limitations in the HG design that produced significant asymmetries.

The primary goal of this study is to assess the effects of loading a symmetric cervical HG to two mesio-distally asymmetric molars.

2. Materials and methods

Six 3D finite element models (FE models) were designed of a mesio-distal slice of maxillae (Fig. 2). Each model consisted of cortical and spongy bone, upper first molars (in models 1–5) and right upper first and left upper second molar (in model 6), their PDL, molar bands on teeth, a cervical HG with symmetric outer bows (Fig. 2). The only differences in the models were in the antero-posterior position of the molars and the inner bow of the HG to adapt their positions (Fig. 3). The molars were in symmetric position in model 1. Models 2–4 showed various amounts of right side molar mesial displacement (0.5 mm, 1.0 mm, 1.5 mm, and 2 mm, respectively). The sixth model showed a specific situation of adjusting the inner bow on the right side first molar and the left side second molar, simulating a case with pre-extraction of the left side first molar.

The models were designed in SolidWorks 2011 (300 Baker Ave. Concord, Masachusetts 01742 USA) and then transferred to ANSYS Workbench Ver. 12.1 (Southpointe, 275 Technology Drive, Cononsburg PA 15317, USA) for the solving process. Meshing was done by the powerful meshing program in the Workbench. Meshed models contained 65303 nodes and 37815 elements (Fig. 2).

The anterior and posterior surfaces of each model were restrained. The end surfaces of outer bows were loaded with a 3 N force. The mechanical properties of the materials used (linear and homogenous) were considered as presented in Table 1. Forces and moments produced in both side molars at different mesio-distal locations were evaluated by FEM.

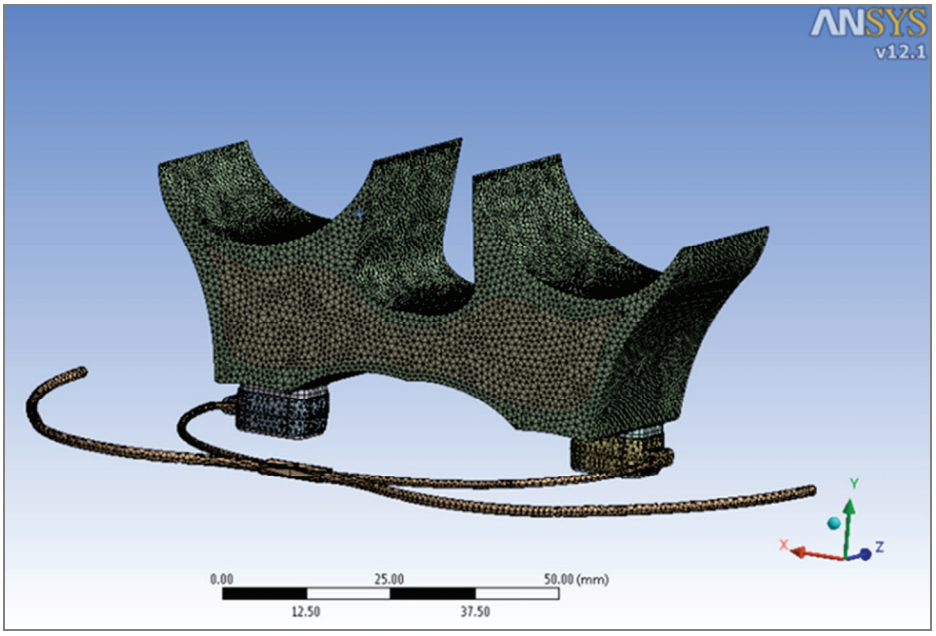

Fig. 2. The 3D meshed model; a mesio-distal slice of the maxillae containing right upper first molar, left upper second molar, their PDLs, cortical bone, spongy bone, a cervical HG, bands fitted on the molars crowns

Table 1. Mechanical properties of the materials used in this study

	Young's modulus (MPa)	Poisson's ratio
Tooth	20300	0.26
PDL	0.667	0.49
Spongy bone	13400	0.38
Cortical bone	34000	0.26
Stainless steel	200000	0.30

3. Analytical solution for a mesio-distal asymmetric molar position in the HG

Let us consider the general case of the circular rod loaded by external distributed and pointed forces and moments of forces (Fig. 3). Bend of a rod (or beam) with a circular axis is considered using the following assumptions [18]:

(1) one of the main axes of the cross-sectional inertia is in the plane of the circular rod;
(2) the rod is inextensible (its length is constant);
(3) the hypothesis of a flat normal is applicable;
(4) cross-sections of the rod are not deformed by applied forces;
(5) deformations of the rod are small;
(6) the rod is thin, i.e., $R/H > 5$ where h and R are the beam thickness and the radius of curvature of the symmetry axis (Fig. 4).

The approach has been successfully used for biomechanical analysis of the symmetric HG [4], [15], [17], the HG with asymmetric outer [3] and inner [22] bows. Using assumptions (1)–6) the equations governing the bend of the rod in the plane of its curvature are [18]

$$\frac{dN}{d\varphi}+Q+pR=0, \qquad \frac{dQ}{d\varphi}-N-qR=0,$$

$$\frac{dM}{d\varphi}+QR-mR=0, \quad M=-\frac{EJ}{R}\frac{d\vartheta}{d\varphi},$$

$$\vartheta=\frac{1}{R}\left(\frac{dw}{d\varphi}+v\right), \qquad w=\frac{dv}{d\varphi},$$

where φ is the angular coordinate of the cross-section; M, N, Q are bending moment of force, normal and cross forces; m, q, p are distributed bending moment of force per unit length and normal and tangent components of external distributed loads; ϑ, w, v are angle of rotation and radial and tangent components of displacements of the cross-section; E is Young's modulus; J is the moment of inertia.

The boundary conditions for (1) must be determined at the ends $\varphi = 0$ and $\varphi = \varphi^k$ of the rod depending on the fastening conditions (Fig. 4). If the external radial P_i and tangent T_i point forces and the point moment of force L_i are applied in the cross sections with angular coordinates $\varphi = \varphi_i$, $i = 1, 2, \ldots$ (Fig. 3), one must integrate (1) between the cross-sections with point loads independently and then compute the general solution using three continuity conditions for

displacements and three more first-order discontinuity conditions for the internal forces and moments of forces at $\varphi = \varphi_i$.

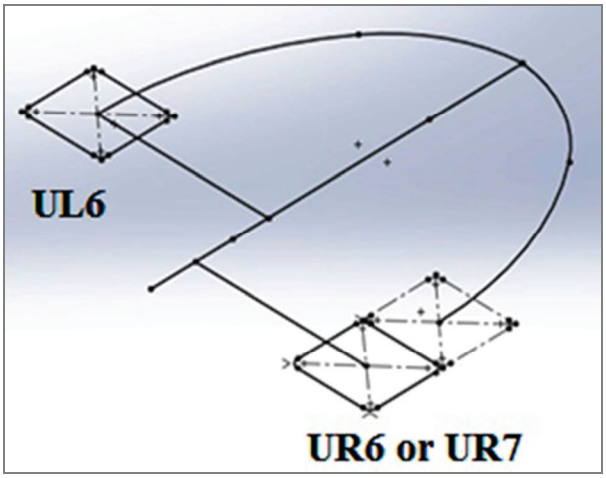

Fig. 3. A general view on the loading of two molars with different mesio-distal locations. The upper left first molar (UL6) is considered to have a normal location in the dental arch. The displaced upper right first molar (UR6) or the upper second molar (UR7) are loaded with a symmetric cervical HG

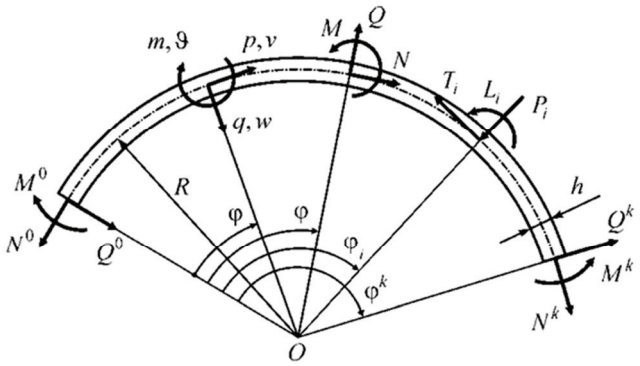

Fig. 4. Circular rod coordinates and forces. A sketch

Using the method of initial parameters [18] for the case of non-zero point forces and moments one can write down the solution of problem (1) for the forces, moment of force and displacements in the form

$$Q = Q^0 \cos\varphi + N^0 \sin\varphi + \sum_{i:\varphi\ge\varphi_i} P_i \cos(\varphi-\varphi_i) + \sum_{i:\varphi\ge\varphi_i} T_i \sin(\varphi-\varphi_i) + Q^*,$$

$$N = -Q^0 \cos\varphi + N^0 \cos\varphi - \sum_{i:\varphi\ge\varphi_i} P_i \sin(\varphi-\varphi_i) + \sum_{i:\varphi\ge\varphi_i} T_i \cos(\varphi-\varphi_i) + N^*,$$

$$M = M^0 - Q^0 R\sin\varphi - N^0 Rc_1(\varphi) + \sum_{i:\varphi\ge\varphi_i} L_i - \sum_{i:\varphi\ge\varphi_i} P_i R\sin(\varphi-\varphi_i) - \sum_{i:\varphi\ge\varphi_i} T_i Rc_i(\varphi-\varphi_i) + M^*, \quad (1)$$

$$\vartheta = \vartheta^0 - \frac{R}{EJ}[M^0\varphi - Q^0 Rc_1(\varphi) - N^0 Rc_2(\varphi) + \sum_{i:\varphi\ge\varphi_i} L_i(\varphi-\varphi_i) - \sum_{i:\varphi\ge\varphi_i} P_i Rc_1(\varphi-\varphi_i) - \sum_{i:\varphi\ge\varphi_i} T_i Rc_2(\varphi-\varphi_i)] - \vartheta^*, \quad (2)$$

$$v = v^0\cos\varphi + w^0\sin\varphi + \vartheta^0 Rc_1(\varphi) - \frac{R^2}{EJ}[M^0 c_2(\varphi) - Q^0 Rc_3(\varphi) - N^0 Rc_4(\varphi) + \sum_{i:\varphi\ge\varphi_i} L_i c_2(\varphi-\varphi_i) - \sum_{i:\varphi\ge\varphi_i} P_i Rc_3(\varphi-\varphi_i) - \sum_{i:\varphi\ge\varphi_i} T_i Rc_4(\varphi-\varphi_i)] - v^*,$$

$$w = -v^0\sin\varphi + w^0\cos\varphi + \vartheta^0 R\sin\varphi - \frac{R^2}{EJ}[M^0 c_1(\varphi) - Q^0 Rc_5(\varphi) - N^0 Rc_3(\varphi) + \sum_{i:\varphi\ge\varphi_i} L_i c_1(\varphi-\varphi_i) - \sum_{i:\varphi\ge\varphi_i} P_i Rc_5(\varphi-\varphi_i) - \sum_{i:\varphi\ge\varphi_i} T_i Rc_3(\varphi-\varphi_i)] + w^*.$$

where

$$c_1(\varphi) = 1-\cos\varphi, \quad c_2(\varphi) = \varphi - \sin\varphi,$$

$$c_3(\varphi) = 1-\cos\varphi - \frac{1}{2}\varphi\sin\varphi,$$

$$c_4(\varphi) = \varphi - \frac{3}{2}\sin\varphi + \frac{1}{2}\varphi\cos\varphi, \quad (3)$$

$$c_5(\varphi) = \frac{1}{2}\sin\varphi - \frac{1}{2}\varphi\cos\varphi.$$

Here, the subscript 0 denotes the corresponding values in the cross-section $\varphi = 0$, while * denotes partial solutions of non-uniform equations (1) produced by the distributed loads only.

Then, six unknown values Q^0, N^0, M^0, ϑ^0, v^0, w^0 in (2)–(3) can be determined from six boundary conditions at $\varphi = 0$, $\varphi = \varphi^k$.

4. A case study for asymmetric load by a point force

Based on the above general theory let us consider the axisymmetric bend of the rod only produced by a pointed force P applied in the vertical direction (Fig. 5). Then the distributed forces in (1) and the corresponding internal forces and moments in (2) are

$$q = 0, \quad p = 0, \quad m = 0, \tag{4}$$

$$T_i = 0, \quad L_i = 0, \quad P_i = P, \quad \varphi_i = \varphi_P. \tag{5}$$

The rigid attachment conditions are applied to the ends of the rod

$$\begin{gathered} w(0) = 0, \quad v(0) = 0, \quad \vartheta(0) = 0, \\ w(\varphi^k) = 0, \quad v(\varphi^k) = 0, \quad \vartheta(\varphi^k) = 0. \end{gathered} \tag{6}$$

Substituting (4) and (5) in (2) gives the following form of solution

$$Q = Q^0 \cos\varphi + N^0 \sin\varphi + P\cos(\varphi - \varphi_P),$$

$$N = -Q^0 \sin\varphi + N^0 \cos\varphi - P\sin(\varphi - \varphi_P),$$

$$M = M^0 - Q^0 R\sin\varphi - N^0 Rc_1(\varphi) - PR\sin(\varphi - \varphi_P),$$

$$\vartheta = \vartheta^0 - \frac{R}{EJ}$$

$$\cdot[M^0\varphi - Q^0 Rc_1(\varphi) - N^0 Rc_2(\varphi) - PRc_1(\varphi - \varphi_P)], \tag{7}$$

$$v = v^0\cos\varphi + w^0\sin\varphi + \vartheta^0 Rc_1(\varphi) - \frac{R^2}{EJ}[M^0 c_2(\varphi)$$

$$- Q^0 Rc_3(\varphi) - N^0 Rc_4(\varphi) - PRc_3(\varphi - \varphi_P)],$$

$$w = -v^0\sin\varphi + w^0\cos\varphi + \vartheta^0 R\sin\varphi - \frac{R^2}{EJ}[M^0 c_1(\varphi)$$

$$- Q^0 Rc_5(\varphi) - N^0 Rc_3(\varphi) - PRc_5(\varphi - \varphi_P)].$$

Substituting (7) in (6) the following result can be obtained

$$\vartheta^0 = 0, \quad v^0 = 0, \quad w^0 = 0, \tag{8}$$

$$\begin{cases} M^0\varphi^k - Q^0 Rc_1(\varphi^k) - N^0 Rc_2(\varphi^k) = PRc_1(\varphi^k - \varphi_P), \\ M^0 c_2(\varphi^k) - Q^0 Rc_3(\varphi^k) - N^0 Rc_4(\varphi^k) = PRc_3(\varphi^k - \varphi_P), \\ M^0 c_1(\varphi^k) - Q^0 Rc_5(\varphi^k) - N^0 Rc_3(\varphi^k) = PRc_5(\varphi^k - \varphi_P), \end{cases} \tag{9}$$

where (9) is the system of linear equations whose coefficients are independent of both E and J.

The solution of (9) is

$$\begin{aligned} \overline{Q}^k &= Q^0\cos\varphi^k + \overline{N}^0\sin\varphi^k + \cos(\varphi^k - \varphi_P), \\ \overline{N}^k &= -\overline{Q}^0\sin\varphi^k + \overline{N}^0\cos\varphi^k - \sin(\varphi^k - \varphi_P), \\ \overline{M}^k &= \overline{M}^0 - \overline{Q}^0\sin\varphi^k - \overline{N}^0 c_1(\varphi^k) - \sin(\varphi^k - \varphi_1), \end{aligned} \tag{10}$$

where the following non-dimensional variables are introduced

$$\overline{Q}^0 = \frac{Q^0}{P}, \quad \overline{N}^0 = \frac{N^0}{P}, \quad \overline{M}^0 = \frac{M^0}{PR}, \tag{11}$$

$$\overline{Q}^k = \frac{Q^k}{P}, \quad \overline{N}^k = \frac{N^k}{P}, \quad \overline{M}^k = \frac{M^k}{PR}. \tag{12}$$

Expression for the displacements w, v and angulation ϑ of the rod can be easily obtained by substituting (10) in three last expressions (7).

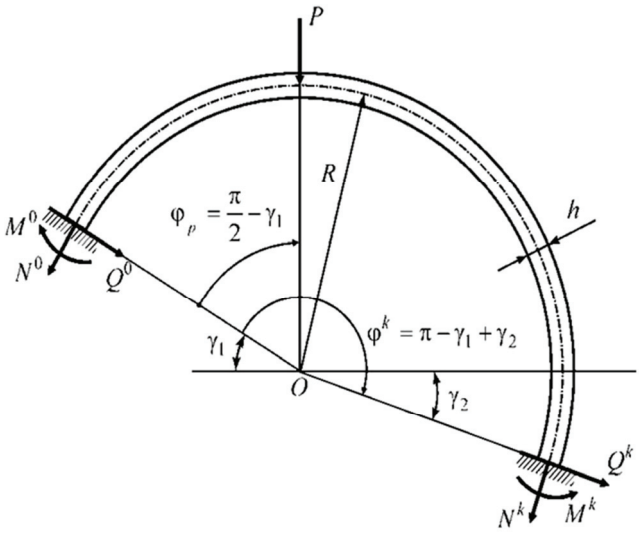

Fig. 5. The circular rod loaded by the point force applied at the top of the rod

5. Results

Numerical computations on (10) of the normal and tangential components of reaction forces and bending moments have been carried out for the non-dimensional values at different angles γ_1, γ_2 = 3, ..., 12 (Fig. 5). The results are presented in Figs. 6–8. Since the non-dimensional reaction forces and moments are independent of both E, J, the applied force P is the only important parameter for numerical computations.

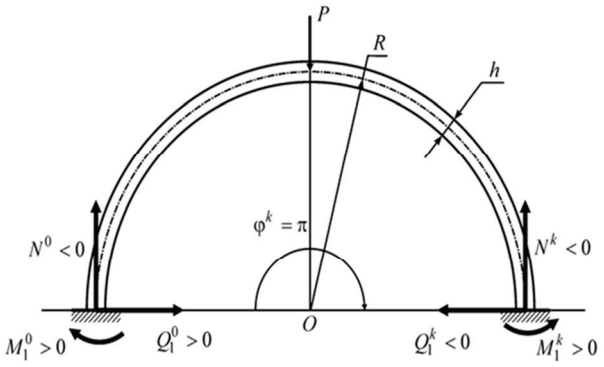

Fig. 6. Symmetric case of the loaded circular rod

The non-dimensional transverse forces computed in the cross-section $\varphi = 0$ and $\varphi = \varphi^k$ (Fig. 5) are presented in Figs. 7a and 7b accordingly. The curves 1–5 correspond to different values of γ_1: $\gamma_1 = 0$ (curve 1), $\gamma_1 = 3°$ (curve 2), $\gamma_1 = 6°$ (curve 3), $\gamma_1 = 9°$ (curve 4), $\gamma_1 = 12°$ (curve 5). The normal components of the forces and the bending moments are presented in Fig. 8a, b and Fig. 9a, b correspondingly. Numeration of the curves in Figs. 8, 9 is the same as in Fig. 7a, b.

The general mechanical theory allows estimation of the main regularities and tendencies in the dependencies of the forces and moments of forces produced

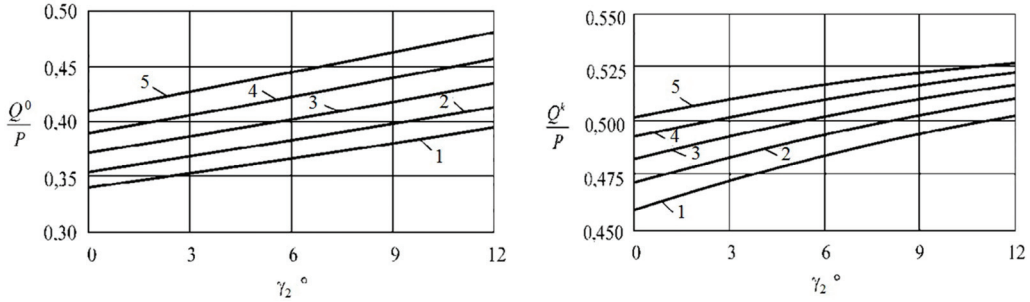

(a) (b)

Fig. 7. The non-dimensional transverse forces at the shorter (a) and longer (b) inner bows

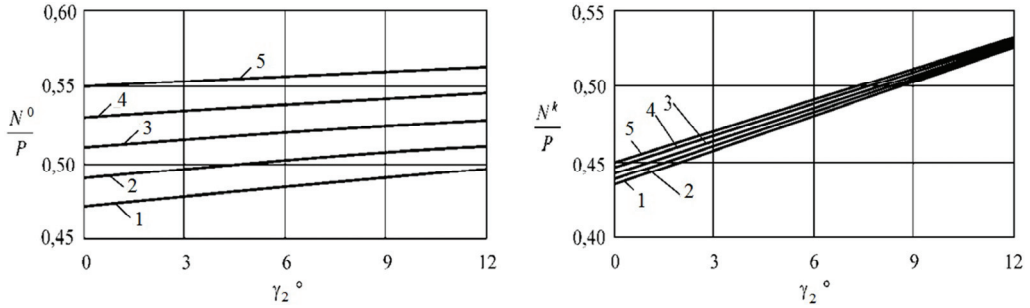

(a) (b)

Fig. 8. The non-dimensional normal forces at the shorter (a) and longer (b) inner bows

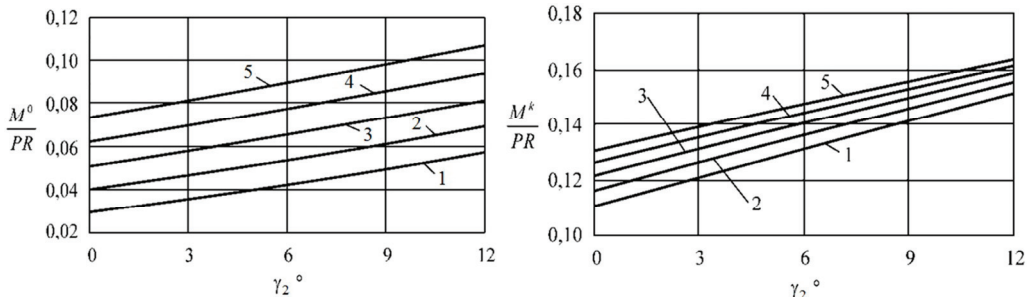

(a) (b)

Fig. 9. The bending moment at the shorter (a) and longer (b) inner bows

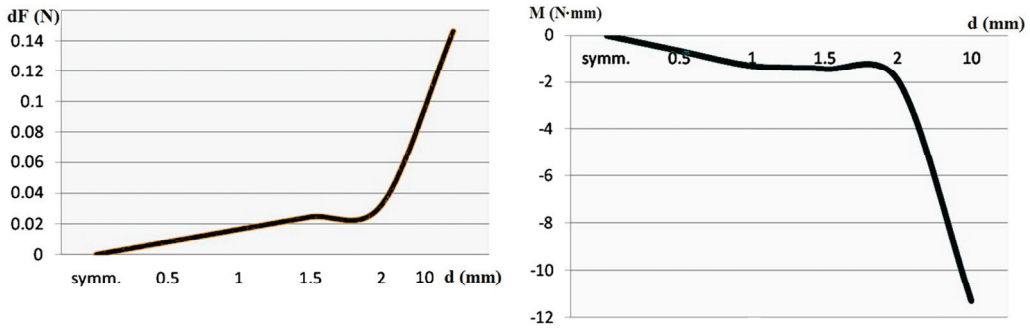

(a) (b)

Fig. 10. Dependence of the difference in the normal forces dN (a) and net moment of force M (b) on the displacement *d* (mm) of the right molar

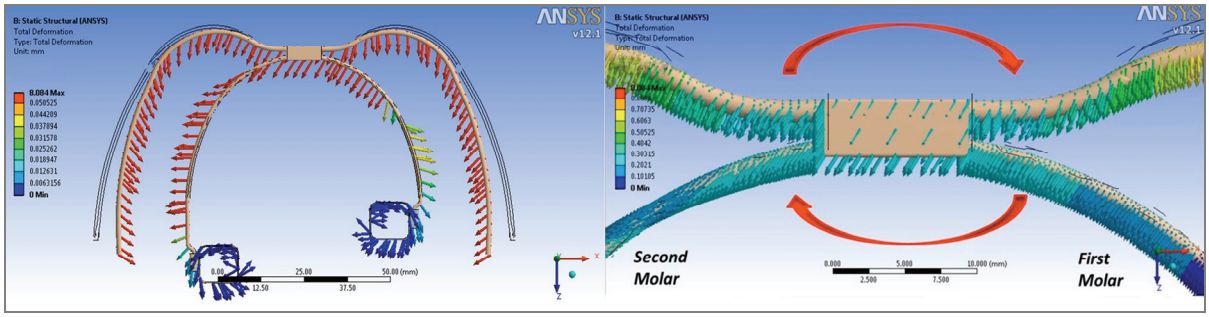

(a) (b)

Fig. 11. Total deformation field in the HG and molars from the top (a) and front (b) views

at the asymmetric inner bow upon symmetric loading of the outer bow at different asymmetric locations of the molars. The more detailed information taking into account 3D geometry of the molars, complex structure of the surrounding tissues and their elastic properties can be obtained by FEM analysis for a case study. The results of 3D FEM computations of the difference in the normal forces dF acting at the shorter and longer inner bows and the net moment of force dM are presented in Fig. 10a and Fig. 10b accordingly. The results computed on the six models described in Section 2 have been approximated by smooth curves. The notifications for the force and moment differ from the notifications in the 2D model, because in the 3D model the net forces and bending moments have been computed over the entire molars. The computations have been carried out with material parameters presented in Table 1 and, therefore the results are obtained in the dimension form, in N for the forces and in N·mm for the bending moments. In this way, the maximal force in Fig. 10a corresponds to the weight of 15 g. For the more detailed illustration of the FEM computations, the displacement fields produced in the HG and on the two molars in model 6 are presented in Fig. 11a, b. The top view on the HG and molars (Fig. 11a) and the enlarged front view of the HG (Fig. 11b) demonstrate all the details of the displacements produced by the force applied to the HG.

6. Discussions

In the case of a symmetric rod (Fig. 6) the obtained numerical results correspond to the well-known analytical solution [18] (see Table 2). The asymmetry in the location of two molars increases with increasing both g1 and g2 values. The transversal force produced

Table 2. Correspondence of numerical computations to known results [25]

Reaction forces	Computations from [25]	Own results	Relative errror %
$\frac{Q^0}{P}, \frac{Q^k}{P}$	0.4551	0.4591	0.88
$-\frac{N^0}{P}, -\frac{N^k}{P}$	0.5	0.5	0
$-\frac{M^0}{PP}, -\frac{M^k}{PR}$	0.1065	0.1106	3.85

by unit load increases with g1 and g2 almost linearly (Fig. 7a) and increases in 17% when g2 goes from 0° to 12°. Similar behavior has been found for the transversal force acting on the long-side molar (Fig. 7b). The force is aimed towards the mid-sagittal line and produce displacement of the molar in the palatal direction. The dependencies of Q^k on g1 and g2 are nonlinear and the force difference between the symmetric and maximal asymmetric geometries is 15%.

The normal component of the forces acting on the short-side and long-side molars also demonstrate monotonous growth with g1 and g2 (Fig. 8a, b), though at the long-side molar the force depends on the position of the molar that increases the arm of force transducing the unit force applied along the mid-sagittal line, and only slightly depends on location of the short-side molar. The maximal force differences at the short-side and the long-side molars are 21% and 18% correspondingly.

The two components of forces will produce complex asymmetric displacement of the molars into the palatal-distal direction. Both transversal and normal components generated by unit force are of the same value varying between 0.34 and 0.55 (Figs. 7, 8). When typical load P = 3–10 N is applied to the HG, the generated forces will exceed the minimal critical values sufficient to produce displacements of the molars [24].

The bending moments acting at the short-side and long-side molars also monotonously increase with increasing asymmetry in the location of both molars (Fig. 9 a,b), though the moment in the long-side part of the HG mostly depends on variation of g2 that increases the torque transferred by the longer arm. Variations in the moment of force at the short-side and long-side molars are 23–95% and 27–36% correspondingly. The computed moments will produce symmetric relating to the mid-lateral line outerwards (negative N^0 and N^k values) rotation of the molars.

The results of 3D FEM computations on the six models described in Sections 2 revealed regularities similar to the foregoing results of 2D analysis. With an increase of the location of the right molar the differences in the forces acting on the long-side and short-side molars increase noticeably (Fig. 10), especially for the high asymmetry (model 6). The distal component of force was the same in model 1 (2.9384 N). The force difference between the intact and displaced molar started with 0.0082 N in 0.5-mm mesio-distal difference and increases gradually to 0.0324 N in a 2-mm mesio-distal difference model. The dF reaches its highest value 0.146 N in the 10-mm difference case (adjusting the HG at UL6 and UR7) and reached 0.146 N. The force difference increases almost linearly with d when $d \in [0; 0.5]$, while the net moment of force exhibits more non-linear behavior.

The net moments were the same in both side molars in the symmetric model, thus producing no net difference moment. A difference was shown to exist between the right and left side molar moments and the important difference of yaw moments was detected (Fig. 10b). This net moment was –0.646 N·mm in a 0.5-mm difference HG design. The negative sign shows a clockwise moment that tends to rotate the system when viewed supero-inferiorly. The net moment increases in accordance with the increased mesio-distal difference of the molar positions and reached –1.945 N·mm in a 2-mm difference. The highest one was –11.32 N·mm in model 6 (Fig. 10b). The 3D computational results are in agreement with more general 2D numerical results, though in the 2D model the bending moment appeared, while in the 3D model three components resulting in a complex rotation were estimated as value of vector of the moment of force.

The total deformations of the HG and molars produced by the net forces and moments are presented in Fig.11a. The outer bow is loaded symmetrically while the inner bow is overloaded at its long-side and significant axisymmetric rotation of the molars in the outer direction is present, as it was noticed on the 2D model. At the applied force of 3N the rotation is relatively small and its appearance will be more important at higher loads of 10 N.

The most important finding of the FEM analysis is a clock-wise yaw moment appearing at symmetric outer load of the asymmetric inner bow (UL6 and UR7 molars). The yaw moment is shown in Fig. 11b by red arrows. The values estimated for the most asymmetrical case showing a 3D rotation out of the plane of the dental arch can destroy the planned orthodontic movement procedure.

In daily dental practice, molars with small amounts of anterior-posterior difference are usually ignored; at least, up to the point with different amounts of molar distalization which is not part of the treatment plan. Generally, when asymmetric HGs are not considered for the treatment, the exact molar relations to the anterior reference plane, which can be considered to pass through the anterior point of the dental arch are not assessed. The decision of usage an asymmetric HG is based on the molar relationship and the individual probable to be improved during the treatment. When dealing with an acceptable molar relationship, a symmetric HG may be used; needless to say that the mesio-distal position of molars relatively to each other is not usually examined. In this way, the asymmetry in the molars locations may mislead the practitioner.

Dealing with class I, molar relation in both sides does not necessarily mean the same mesio-distal position of the molars, which is a precondition for the symmetry of the system. It may have been produced by a simultaneous mesial shift of the upper and lower molars in one side of the arch or different mesio-distal widths of the left and right side teeth. In some situations, the molar relation is not a perfect class I, but is accepted as a suitable one to avoid the side effects of prescribing an asymmetric HG.

Our knowledge about using a symmetric cervical HG was limited to having a distal driving and extrusive force when viewed occlusally [18], [19]. It is limited by a force system where the symmetric plane of the HG and the terminal molar plane are perpendicular to each other. The force vector when analyzed in combination with the moment difference (Fig. 10b) present in the system can produce different molar distal movements in both sides of the arch. A residual moment was shown rotating the dental arch clockwise when viewed superior-inferiorly. The clockwise/counterclockwise manner of rotation is decided by the position of the molars involved. If the mesial molar is in the right side, the rotation will be clockwise and vice versa. (Figs. 11a, b). Combining the effects of right and left force systems variance and the residual moment, a prediction of the final position of the molars may be elusive.

The inner bow wire between the inner/outer bow connection and the terminal molars on both sides are normally not the same. The difference in the wire lengths provides different bending in both sides of the inner bow [7]. This starts from few tenths of millimeters to few millimeters when considering a case with unilateral extracted first molar.

Without perfect symmetry the traction force is not divided equally between the terminal molars. This can cause different amounts of distal tipping and rotation around vertical axes. Thus, considering the net moment described, a tendency for mesio-buccal movement of the distally positioned molar and a tendency for mesio-palatal movement of the mesially positioned molar due to the system rotation can be expected. In this way, the efficiency of the cervical HG in distalizing molars is reduced.

FEM was shown an acceptable method of detailed computations of the forces, moments and deformations on the individual geometry and biomechanical substantiation of necessity of symmetric or asymmetric HG in each case. The medio-lateral discrepancy of the left vs. the right molars, in conjunction with the mesio-distal discrepancy, can make the resulting tooth movement more complex.

A discrepancy in molar position is often ignored in a medio-lateral direction and may also be ignored in an antero-posterior direction. Mesial movement of the molar can occur with or without displacement towards mid-palatal area. If both displacements occur, the force received by the medial one will be larger than the farther one [5]. This medial movement is due to the arch form and the dominant pattern of the molar movement in the upper jaw which occurs by a rotation around the palatal root. In this study, the probable medial displacement of the molar combined with its anterior movement is ignored to make the analysis simple.

A symmetroscope can be employed to evaluate the molars' position. Based on the present study, to reduce the side effects of HGs it is strongly recommended to correct the position of molars before starting HG therapy (e.g., palatal bars and their modifications). Unilateral extended palatal bars can help in treating malposition of the molars. The symmetroscope is also suggested to be used in assessing the inner bow form at the end of adjustment. Some of the asymmetries made in the process of adjustment can be easily corrected.

In this way, two different distal forces were produced without any lateral driving component. It is the difference between the force system of an asymmetric HG produced by different outer bow lengths and the one produced by the mesio-distal different positions of the molars when loaded by a symmetric HG. Again, analyses elucidated that processes may be more complex than it was expected.

The findings of this study involve light forces which are often ignored. Since light forces efficiently moving a tooth with as little as two grams weight are well known [24], how can we ignore it in molars loaded by a cervical HG? In this way, preliminary biomechanical analysis based either on the 2D model allowing fast preliminary estimations or on more detailed 3D geometry dependent model which needs more time for the model preparation and FEM computations, is shown to be an important component of the daily dental practice.

7. Conclusions

1. The process of clinical application and adjustment of HGs is complex and should be looked at thoroughly in detail.
2. Different components of distal force were shown to exist when molars are located in different an-

tero-posterior positions. The mesial side molar receives more distalizing force than the distal one.

3. A residual yaw moment was shown to exist tending to rotate the whole system clockwise/counter clockwise when viewed superior-inferiorly.

References

[1] ARMSTRONG M.M., *Controlling the magnitude, direction, and duration of the extra oral force*, Am. J. Orthod., 1971, 59, 217–243.

[2] BONDEMARK L., KARLSON I., *Extraoral vs intraoral appliance for distal movement of maxillary first molar: a randomized controlled trial*, Angle Orthod., 2005, 75, 699–706.

[3] BROSH T., PORTAL S., SARNE O., VARDIMON A.D., *Unequal outer and inner bow configurations: comparing 2 asymmetric headgear systems*, Am. J. Orthod. Dentofacial Orthop., 2005, 128, 68–75.

[4] CONTASTI G.A., LEGAN H.L., *Biomechanical guidelines for the headgear application*, J. Clin. Orthop., 1982, 16, 308–312.

[5] GERAMY A., *Cervical head gearforce system: 3D analysis using finite element method*, Journal of Dentistry, Shiraz Univ. of Medical Sci., 2000, 2, 21–30.

[6] GERAMY A., HASSANPOUR M., EMADIAN R.E., *Asymmetric outer bow length and cervical headgear force system: 3D analysis using finite element method*, Journal of Dentistry, Tehran University of Medical Sciences, 2015, 12, 216–225.

[7] GERAMY A., KIZILOVA N., TEREKHOV L., *Finite element method (FEM) analysis of the force systems produced by asymmetric inner head gear bows*, Austr. Orthod. J., 2011, 27, 125–131.

[8] GERAMY A., MORTEZAI O., ESMAILY M., DARVISHPOUR H., *Unilateral outer bow expanded cervical headgear force system: 3D analysis using finite element method*, J. Dentistry, Tehran University of Medical Sciences, 2015, 12, 271–280.

[9] GODT A., KALWITZKI M., GOZ G., *Effects of cervical head gear on overbite against the background of existing growth pattern. A retrospective analysis of study casts*, Angle Orthod., 2007, 77, 42–46.

[10] GOULD I.E., *Mechanical principles in extra oral anchorage*, Am. J. Orthod., 1957, 43, 319–333.

[11] GRABER T.M., *Extra oral force-Facts and Falacies*, Am. J. Orthod., 1955, 41, 490–505.

[12] GREENSPAN R.A., *Reference charts for controlled extra oral force application to the maxillary molars*, Am. J. Orthod., 1970, 58, 486–491.

[13] HAACK D.C., WEINSTEIN S., *The mechanics of centric and eccentric cervical traction*, Am. J. Orthod., 1958, 44, 346–357.

[14] HAYDER S., UNER O., *Comparison of Jones Jig molar distalization appliance with extraoral traction*, Am. J. Orthod. Dentofacial Orthop., 2000, 117, 49–53.

[15] HERSHEY H.G., HOUGHTON C.W., BURSTONE C.J., *Unilateral face bows: A theoretical and laboratory analysis*, Am. J. Orthod. Dentofacial Orthop., 1981, 79, 229–249.

[16] JACOBSON A., *A key to the understanding of extra oral forces*, Am. J. Orthod., 1979, 75, 361–386.

[17] KUBEIN-MEESENBURG D., JAGER A., BORMANN V., *Kloehn headgear force analysis*, J. Clin. Orthod., 1984, 18, 882–890.

[18] MARCOTTE M.R., *Biomechanics in orthodontics*, B.C. Decker Inc., Toronto, 1990.

[19] NIKOLAI R.J., *Bioengineering analysis of orthodontic mechanics*, Lea &Febiger, Philadelphia, 1985.

[20] OOSTHUIZEN L., DIJKMAN J.F.P., EVAN W.G., *A mechanical appraisal of the Kloehn extra oral assembly*, Am. J. Orthod., 1973, 43, 221–232.

[21] SANDUSKY W.C., *Cephalometric evaluation of the effects of the Kloehn type of cervical traction used as an auxiliary with the edgewise mechanism following Tweed's principle for correction of class II div.1 malocclusion*, Am. J. Orthod., 1965, 51, 262–287.

[22] SQUEFF L.R., RUELLAS A.C., PENEDO N.D. et al., *Asymmetric headgear for differential molar movement: a study using finite element analysis*, J. Orthod., 2009, 36, 145–151.

[23] USUMEZ S., ORHAN M., UYSAL T., *Effect of cervical headgear wear on dynamic measurement of head position*, Eur. J. Orthod., 2005, 27, 437–442.

[24] WEINSTEIN S., *Minimal forces in tooth movement*, Am. J. Orthod., 1967, 53, 881–903.

[25] WORMS F.W., ISAACSON R.J., SPEIDLE T.M.A., *Concept and classification of rotation and extra oral force systems*, Am. J. Orthod., 1973, 43, 384–401.